

# Quantifying the Infected Population for Calibrated Intervention and Containment of the COVID-19 Pandemic

Liang Tian<sup>1,2,#</sup>, Xuefei Li<sup>1,3,#</sup>, Fei Qi<sup>1,3</sup>, Qian-Yuan Tang<sup>1,4</sup>, Viola Tang<sup>1,5</sup>, Jiang Liu<sup>1,6</sup>, Xingye Cheng<sup>1,2</sup>, Xuanxuan Li<sup>1,7,8</sup>, Yingchen Shi<sup>1,7,8</sup>, Haiguang Liu<sup>1,8,9</sup>, Lei-Han Tang<sup>1,2,8,\*</sup>

#Contributed equally

<sup>1</sup>COVID-19 Modelling Group, Hong Kong Baptist University, Kowloon, Hong Kong SAR, China, <http://covid19group.hkbu.edu.hk>

<sup>2</sup>Department of Physics and Institute of Computational and Theoretical Studies, Hong Kong Baptist University, Kowloon, Hong Kong SAR, China

<sup>3</sup>CAS Key Laboratory of Quantitative Engineering Biology, Shenzhen Institute of Synthetic Biology, Shenzhen Institutes of Advanced Technology, Shenzhen 518055, China

<sup>4</sup>Center for Complex Systems Biology, Universal Biology Institute, University of Tokyo, 113-0033 Tokyo, Japan

<sup>5</sup>Department of Information Systems, Business Statistics and Operations Management, Hong Kong University of Science and Technology, Hong Kong SAR, China

<sup>6</sup>Scarsdale, NY 10683, USA

<sup>7</sup>Department of Engineering Physics, Tsinghua University, Haidian, Beijing 100084, China

<sup>8</sup>Complex Systems Division, Beijing Computational Science Research Center, Haidian, Beijing 100193, China

<sup>9</sup>Physics Department, Beijing Normal University, Haidian, Beijing 100875, China

\*Correspondence: [lhtang@hkbu.edu.hk](mailto:lhtang@hkbu.edu.hk), Lei-Han Tang, Department of Physics, Hong Kong Baptist University, Hong Kong SAR, China

## Abstract

The COVID-19 has infected more than 462,000 people globally and resulted in over 20,000 deaths as of March 26, 2020 <sup>1,2</sup>. Swift government response to contain the outbreak requires accurate and continuous census of the infected population, particularly with regard to viral carriers without severe symptoms <sup>3-8</sup>. We take on this task by converting the symptom onset time distribution, which we calibrated, into the percentage of the latent, pre-symptomatic and symptomatic groups through a novel mathematical procedure. We then estimate the reduction of the basic reproduction number  $R_0$  under specific disease control practices such as contact tracing, testing and social distancing. Finally, in light of our model findings, we analyze the bell-shaped curves of epidemic evolution from various affected regions, and recommend measures to steer the pandemic to its final descent at a universal decay rate of  $-0.32/\text{day}$ .

**Keywords:** COVID-19, Disease transmission model, Pre-symptomatic, Epidemic evolution and control.

The Coronavirus Disease 2019 (COVID-19) is a new contagious disease caused by the novel coronavirus (SARS-CoV-2)<sup>9</sup>, which belongs to the genera of *betacoronavirus*, the same as the coronavirus that caused the SARS epidemic between 2002 and 2003<sup>10</sup>. COVID-19 has spread to more than 170 countries, infected more than 462,000 people and claimed over 20,000 lives as of March 26, 2020<sup>1</sup>. The outbreak has been declared a pandemic and a public health emergency of international concern<sup>2</sup>. Given its enormous span over a great variety of communities and nations, data from all sources are needed to formulate successful intervention strategies towards the containment of the disease. At this stage, there exists a wealth of carefully documented clinical data on the disease progression and transmission, which can be mined to construct quantitative models of how individual outbreaks rise and cede. Coupled with a systematic characterization of how the disease has spread within and among different communities, effective intervention measures can be implemented while minimising the associated economic and social costs.

As the specific symptoms of COVID-19 are now well-publicised, symptomatic transmissions are being contained in most countries. However, disease transmission by pre-symptomatic or asymptomatic viral carriers is much harder to deal with due to its hidden nature<sup>4</sup>. Clinical data reveals that viral load becomes significant before the symptom onset<sup>11-13</sup>. The epidemiological investigation has identified cases of pre-symptomatic transmission based on the onset time interval studies<sup>3,7,8,14</sup>. Despite wide-spread public concern, estimates vary greatly among experts on the percentage of total transmission due to this group of viral carriers, ranging from as low as 10% to over 50%<sup>15</sup>. A model-based study by Ferretti et al.<sup>16</sup> suggested that pre-symptomatic transmission alone could yield a basic reproduction number  $R_{0,p} = 0.9$ , close to the critical value of 1.0 that sustains epidemic growth. As the epidemic is driven by the most infectious group at any given period, it is not inconceivable that, as symptomatic transmission loses heat, pre-symptomatic and asymptomatic transmission takes over in fueling the outbreak<sup>4</sup>.

To tackle the myriad of issues and questions regarding the outbreak, a simple quantitative model, based on the essential facts of COVID-19 transmission, is much desired. The model can provide a baseline to put the latest findings in perspective, and to facilitate novel ideas on intervention. In this paper, we show that such a goal is indeed reachable. By transforming the symptom onset time distribution into the reproductive rate since infection, we build a quantitative model that brings out universal features of individual outbreaks. The model allows one to convert the cumulative number of confirmed cases to the current size of the pre-symptomatic population. Subsequently, one can estimate the percentage reduction in the basic reproduction number  $R_0$  (estimated to be around 3.68 at a growth rate of 0.3/day) due to contact tracing carried out within a specific period after infection, with or without testing.

## Model

In epidemiological studies, the key quantity is the average number of infections per unit time  $r(t)$  by a viral carrier who was infected at  $t = 0$ . In the case of COVID-19, disease transmission from a given individual peaks around his/her symptom onset time <sup>12,13</sup>, as illustrated by the infectiousness curve shown in Fig. 1. This property, when averaged over the population, gives an  $r(t)$  that peaks at nearly the same time as the symptom onset time distribution, which we denote by  $p_O(t)$ . In fact, when the time window of transmission is narrow compared to the mean symptom onset time  $\tau_O$ , we have approximately

$$r(t) \approx R_0 p_O(t). \quad (1)$$

Equation (1) forms the basis of our analysis.

To incorporate the actual shape of the infectiousness curve, we developed a more complete model as presented in Supplementary Information. The model splits the pre-symptomatic period into two phases, a non-infectious latent phase L, followed by the infectious pre-symptomatic phase A. For convenience, the infected population is grouped by the symptom phases, denoted as L, A, and S. Starting from infection at  $t = 0$ , an individual first stays in the latent phase L. Transition to phase A takes place at a rate  $\alpha_L(t)$ , which increases with  $t$ . Once in phase A, the individual develops symptoms and enters the symptomatic S phase at a rate  $\alpha_A$ , independent of how long the person has been in phase A. The mean duration of phase A is given by  $\alpha_A^{-1}$ , chosen to correspond to the size of the left wing of the infectiousness curve. Transmission rate in phase A is set by  $\beta_A$ . Once in S, the person remains in this symptomatic phase, with a disease transmission rate  $\beta_S(\tau)$  that matches the right wing of the infectiousness curve. The total area underneath the infectiousness curve is given by  $R_0 = R_0^A + R_0^S$ , with  $R_0^A = \beta_A / \alpha_A$ , and  $R_0^S = \int_0^\infty \beta_S(t) dt$ . Introducing a parameter  $\beta_{\text{eff}} = \beta_A + \alpha_A R_0^S$ , we have

$$R_0 = \frac{\beta_{\text{eff}}}{\alpha_A}. \quad (2)$$

This completes the specification of our detailed model. In Supplementary Information, we show that the  $r(t)$  of this model can be written in the form of Eq. (1) with a slightly modified onset time distribution. In view of its mathematical simplicity, we will adopt Eq. (1) in the following and leave the more technical discussions to Supplementary Information. Denoting by  $A(t)$  the size of the infected population in phase A in a well-mixed community, we have

$$\dot{A} = -\alpha_A A + \int_{-\infty}^t K(t - t_1) A(t_1) dt_1. \quad (3)$$

with the kernel function given by

$$K(t) = R_0 e^{-\alpha_A t} \frac{d}{dt} [e^{\alpha_A t} p_O(t)]. \quad (4)$$

An obvious advantage of our model, as compared to some of the other epidemic models, is that its parameters have clear physical meaning and thus can be determined directly from clinical case studies. We undertake this task below using available data. By

combining two data sets <sup>8,17</sup> with a total of 159 infection cases, we calibrated the statistical behavior of the symptom onset time as shown in Fig. 2a, and obtained  $\tau_a = 5.17$  days, with a standard deviation of 2.93 days. The data is validated against a serial interval study on 468 infection pairs <sup>3</sup> with excellent consistency (see Supplementary Information). Starting from day 6,  $p_O(t)$  decays exponentially at a rate of  $-0.32/\text{day}$ . As will be elaborated later, this decay rate is the upper bound for the decreasing rate of daily cases when the whole infectious population is fully isolated. The parameter  $\alpha_A$  controls the apparent duration of phase A, but its actual value has only a weak effect on our predictions. In our numerical exploration, we use the estimated value  $\alpha_A \approx 0.75/\text{day}$  based on a data set compiled by Xia et al <sup>8</sup>. The basic reproduction number  $R_0$  is taken as a control parameter in our study.

Figure 2b shows the probabilities that a given individual is in one of the three phases at day  $t$  after infection, computed using the formula in Table S1 (Supplementary Information). The red line marks the boundary between the pre-symptomatic and symptomatic phases. Dashed lines above the red line indicate probabilities that the individual is one day or two days into the symptomatic phase, respectively. The width of the orange region, on the other hand, is proportional to  $\alpha_A^{-1} = 1.5$  days. Shown in Fig. 2c are the Laplace transforms of these curves, yielding the percentage of the infected population in each of the three phases on a given day when the epidemic is growing at a rate  $\lambda$ . These curves allow for estimation of the hidden population in L and A from the knowledge of S in real time. The actual size of S, which includes all individuals who have developed symptoms in the past, regardless of whether they have recovered from the disease, can be estimated from the total number of confirmed cases until that time point. Note that at high growth rates, probabilities at short times in Fig. 2b contribute more to the Laplace transforms, leading to a larger percentage of the total infectious population being constituted by the hidden population.

Under Eq. (1), the well-known Lotka–Euler estimating equation <sup>18</sup> yields,

$$R_0 = \frac{1}{\tilde{p}_O(\lambda)}. \quad (5)$$

where  $\tilde{p}_O(\lambda) = \int_0^\infty p_O(t)e^{-\lambda t} dt$  is the Laplace transform of  $p_O(t)$ . Using our calibrated numbers, we obtain from Eq. (5) the  $R_0$ - $\lambda$  curve shown in Fig. 2d for COVID-19, which covers both growth and decline phases of the epidemic. At the very high growth rate of  $\lambda = 0.3/\text{day}$  seen in China in late January 2020 and now in Europe and the US in March 2020, our estimated value of  $R_0$  is 3.68, which agrees with other studies <sup>6,19–23</sup>. According to Eq. (2),  $R_0$  is proportional to the transmission parameter  $\beta_{\text{eff}}$ . Thus if one is to rely on social distancing alone, the number of close social contacts per individual needs to be reduced to  $R_0^{-1} = 27\%$  of its original level to stop epidemic growth, highlighting the tremendous sacrifice required in the infected communities. The left end of the curve gives an ultimate epidemic decay rate of  $-0.32/\text{day}$  at  $R_0 = 0$ , i.e., a complete eradication of disease transmission.

## Testing and Contact Tracing

To lessen the impact of social distancing practices on the general public, governments have mainly adopted two measures to track COVID-19 transmission: 1) testing and isolating infected individuals; and 2) tracing and quarantining contacts of infected individuals. For testing control, persons who had close contact with a confirmed infection case are asked to undergo voluntary or mandatory testing for infection, and quarantined when the result is positive. From Fig. 2b we see that, if the test is conducted too close to the day of contact, the individual has a high probability to still be in the latent phase, hence the test result is likely to be negative. On the other hand, if the test is conducted too late, the person may have already infected others so that the reduction of  $r(t)$  given by Eq. (1) is small. Therefore, there is an optimal interval between contact date and the test date, which we analysed in the Supplementary Information. Figure 2e shows the function  $g(t) = r(t)/R_0$  without intervention, and in three examples when the test was performed on day 2, day 3 and day 4 after contact, under the best case scenario when all close contacts were traced and test results were immediately available. Relative change of the basic reproduction number  $R_0$  is given by the sandwiched area in each case. In Fig. 2f, we show the reduction of  $R_0$  as a function of the test date after contact for immediate reporting (red line) and delay of result by one day (blue line), with an initial value of  $R_0 = 3.68$ . The best result is obtained when the test is performed on day 4. This corresponds to the day when the width of the orange region in Fig. 2b is the widest. The actual value of 20% reduction when there is no reporting delay depends on the total width of the infectious interval, which should also extend to the symptomatic side if self-quarantine is not assumed. For contact tracing and quarantining, we show our results for aggressive contact tracing under the scenario that all close contacts are traced and quarantined on day  $t$  after contact, without testing the individual for the virus (Fig. 2f). The reduction of  $R_0$  is much greater if full tracing and quarantining are executed within 2-3 days after contact. If tracing is less than 100%, the reduction is compromised proportionally. The above estimation procedure can be generalised to cases when testing or contact tracing are completed within a given period rather than on a particular day in terms of a weighted average of the reductions (see Supplementary Information). These numbers can be used to design optimal strategies that combine social distancing, testing and contact tracing to contain the epidemic in a particular region, taking into account the local political, economic and social situations.

## Three-phase Epidemic Development

From the time-series data of daily confirmed cases of COVID-19 obtained from the Johns Hopkins CSSE Repository<sup>24</sup>, we identify three phases of COVID-19 epidemic development from different places in China following the Wuhan lockdown on January 23, 2020, with universal features at the beginning and end of regional outbreaks. These observations are interpreted within our model setting.

Phase I is characterised by exponential growth of the epidemic. In China, in the first week after the Wuhan lockdown on January 23, 2020, the number of daily confirmed

cases continued to grow at a rate of approximately 0.3/day (Fig. 3a and 3b, dashed-black line), equivalent to an eight-fold increase per week. Data shows that most of the growth during this period is related to infections that can be traced to Hubei province, the epicenter of the initial outbreak. As we explain in the Supplementary Information, the universal growth rate is set by latent, pre-symptomatic and symptomatic viral carriers from Hubei province, whose percentage among these travellers, while still low, grows exponentially in that period. The fraction of local infections can be calculated using our model, and the result depends on the local value of  $R_0$ .

Phase II is a local consolidation or crossover phase where new imported cases have largely ceased due to the lockdown, and when public policies to contain the disease spreading are taking effect. On a logarithmic scale, data from the most affected provinces apart from Hubei show consistent behaviour. Close examination, however, reveals sporadic outbreaks in local communities that vary from province to province. Well-known examples include prison cases in Hubei, Shandong and Zhejiang provinces<sup>25</sup>. Overall, under the swift and forceful implementation of contact tracing, isolation and social distancing policies, turnaround of the epidemic in provinces other than Hubei was reached in about three weeks after the regional lockdown. In Fig. 3b and the supplementary Fig. S4, we present simulation results using our model, assuming a linear decrease of  $R_0$  from a local value of 2.0 to zero over a period  $T$ , which indeed reproduces the bell-shaped curve as seen in Fig. 3. The more gradual change of  $R_0$  assumed in our simulations can be interpreted as due to the progressive government policies including additional lockdowns, which took place from February 4-10<sup>26,27</sup>, as well as the time needed for these policies to take effect in communities that experienced new outbreaks.

Phase III, or the final descent, occurred when the intervention measures essentially eliminated new outbreaks. The few that surfaced were quickly identified and contained. Within our model, the newly confirmed cases in this period are identified with the shrinking number of individuals moving from the latent to the symptomatic phase, as one moves along the time axis in Fig. 2b. Strikingly, the observed decay rate in this phase reached the maximum value of 0.32/day, including data from Hubei province shown in Fig. 3a. This observation indicates that the infected cases were isolated at extremely high efficiency.

We now examine the situation elsewhere in the world. Exponential growth with a daily growth rate of around 0.3 is seen in the latest epidemic data from a number of countries (Fig. 3c). While these outbreaks were initially seeded by imported cases, they are now largely driven by local infections. Under successful interventions, a few countries have transitioned to the crossover phase observed in China in February (Fig. 3d). The government of Italy imposed a national quarantine on March 9<sup>28</sup>, after which growth in the number of newly confirmed cases slowed down<sup>24</sup>. We fit the data after March 9, which yields a growth rate of 0.05/day (Fig. 3d), corresponding to  $R_0 = 1.3$  according to our model, still higher than what is needed to contain the outbreak. On the other hand, South Korea adopted very aggressive contact tracing and testing policies<sup>29,30</sup>, enabling the country to bring the initially rampaging outbreak to a much more manageable level at a  $R_0 \approx 1$  (Fig. 3d, stars). These countries are now facing the

challenge of dealing with import driven growth, which can be analysed using our model (see Supplementary Information).

## Conclusions

We have developed a simple yet powerful model to describe the spread of COVID-19 infection in a well-mixed community, which can be applied to local outbreaks as well as national level epidemics. The effect of intervention measures in a regional setting, such as social distancing, contact tracing, testing and isolation, can be readily incorporated into the model for quantitative assessment and prediction. This is especially useful in the ongoing battle in many countries to bring the pandemic under control. As we demonstrated in this paper, further reduction of the still positive growth rate requires quantitative evaluation of the proposed measures. While the data used to construct the reproduction rate function given by Eq. (1) will continue to be updated, the current predictions should already be informative to decision-makers at all levels in their adoption of effective measures to bring down the pandemic. As the pandemic is fueled by transmission in the fastest growing community, reaching out to all sectors of society will pose the biggest challenge. In this respect, fast and efficient measures to monitor epidemic development will be essential.

An important issue not treated explicitly in this work is the role played by asymptomatic carriers of the virus, i.e., those who never exhibit severe symptoms. We have made the implicit but plausible assumption that the reproduction rate function for this group of infected individuals is weaker or the same as the one given by Eq. (1), in which case their contribution is slaved to the group captured by Eq. (3), without altering the structure of our model. However, aside from imposing general house-confinement, other intervention measures may have a weaker effect in reducing transmission by asymptomatic viral carriers. This urgent issue awaits further study.

## Acknowledgments

The work is supported in part by the NSFC under Grant Nos. 11635002 and U1530402, and by the Research Grants Council of the Hong Kong Special Administrative Region (HKSAR) under Grant Nos. HKBU 12324716.

## Conflict of Interest Statement

Authors declare no conflict of interest.

## Disclaimer

Any views expressed by Jiang Liu and Viola Tang are not as a representative speaking for or on behalf of his/her employer, nor do they represent his/her employer's positions, strategies or opinions.

## References

1. World Health Organization. Coronavirus disease 2019 (COVID-19) Situation Report – 66. (2020).
2. WHO. WHO Director-General's opening remarks at the mission briefing on COVID-19 - 26 February 2020. 1–6 (2020). Available at: <https://www.who.int/dg/speeches/detail/who-director-general-s-opening-remarks-at-the-media-briefing-on-covid-19---11-march-2020>. (Accessed: 13th March 2020)
3. Du, Z. et al. The serial interval of COVID-19 from publicly reported confirmed cases. medRxiv 2020.02.19.20025452 (2020). doi:10.1101/2020.02.19.20025452
4. Anderson, R. M., Heesterbeek, H., Klinkenberg, D. & Hollingsworth, T. D. How will country-based mitigation measures influence the course of the COVID-19 epidemic? *The Lancet* 0, (2020).
5. Hu, Z. et al. Clinical characteristics of 24 asymptomatic infections with COVID-19 screened among close contacts in Nanjing, China. *Sci. China Life Sci.* 1–6 (2020). doi:10.1007/s11427-020-1661-4
6. Mizumoto, K. & Chowell, G. Transmission potential of the New Corona (COVID-19) onboard the Princess Cruises Ship, 2020. *Infect. Dis. Model.* 5, 264–270 (2020).
7. Nishiura, H., Linton, N. M. & Akhmetzhanov, A. R. Serial interval of novel coronavirus (COVID-19) infections. *Int. J. Infect. Dis.* (2020). doi:10.1016/j.ijid.2020.02.060
8. Xia, W. et al. Transmission of corona virus disease 2019 during the incubation period may lead to a quarantine loophole. medRxiv 2020.03.06.20031955 (2020). doi:10.1101/2020.03.06.20031955
9. Zhou, P. et al. A pneumonia outbreak associated with a new coronavirus of probable bat origin. *Nature* 579, 270–273 (2020).
10. Wu, F. et al. A new coronavirus associated with human respiratory disease in China. *Nature* 579, 265–269 (2020).
11. Zou, L. et al. SARS-CoV-2 Viral Load in Upper Respiratory Specimens of Infected Patients. *N. Engl. J. Med.* (2020). doi:10.1056/NEJMc2001737
12. He, X. et al. Temporal dynamics in viral shedding and transmissibility of COVID-19. medRxiv 2020.03.15.20036707 (2020). doi:10.1101/2020.03.15.20036707
13. To, K. K. et al. Temporal profiles of viral load in posterior oropharyngeal saliva samples and serum antibody responses during infection by SARS-CoV-2: an observational cohort study. *Lancet Infect. Dis.* 3099, 1–10 (2020).
14. Huang, R., Xia, J., Chen, Y., Shan, C. & Wu, C. A family cluster of SARS-CoV-2 infection involving 11 patients in Nanjing, China. *Lancet Infect. Dis.* 0,

(2020).

15. Qiu, J. Covert coronavirus infections could be seeding new outbreaks. *Nature* (2020). doi:10.1038/d41586-020-00822-x
16. Ferretti, L. et al. Quantifying dynamics of SARS-CoV-2 transmission suggests that epidemic control and avoidance is feasible through instantaneous digital contact tracing. *medRxiv* 2020.03.08.20032946 (2020). doi:10.1101/2020.03.08.20032946
17. Men, K. et al. Estimate the incubation period of coronavirus 2019 (COVID-19). *medRxiv* 2020.02.24.20027474 (2020). doi:10.1101/2020.02.24.20027474
18. Wallinga, J. & Lipsitch, M. How generation intervals shape the relationship between growth rates and reproductive numbers. *Proc. R. Soc. B Biol. Sci.* 274, 599–604 (2007).
19. You, C. et al. Estimation of the Time-Varying Reproduction Number of COVID-19 Outbreak in China. *medRxiv* 2020.02.08.20021253 (2020). doi:10.1101/2020.02.08.20021253
20. Zhang, S. et al. Estimation of the reproductive number of novel coronavirus (COVID-19) and the probable outbreak size on the Diamond Princess cruise ship: A data-driven analysis. *Int. J. Infect. Dis.* 93, 201–204 (2020).
21. Wang, Y. et al. Estimating the basic reproduction number of COVID-19 in Wuhan, China. *Chinese J. Epidemiol.* 41, 476–479 (2020).
22. Tang, B. et al. The evolution of quarantined and suspected cases determines the final trend of the 2019-nCoV epidemics based on multi-source data analyses. *SSRN eLibrary* (2020).
23. Read, J. M., Bridgen, J. R., Cummings, D. A., Ho, A. & Jewell, C. P. Novel coronavirus 2019-nCoV: early estimation of epidemiological parameters and epidemic predictions. *medRxiv* 2020, 2020.01.23.20018549 (2020).
24. Dong, E., Du, H. & Gardner, L. An interactive web-based dashboard to track COVID-19 in real time. *Lancet Infect. Dis.* 3099, 19–20 (2020).
25. CNBC News. China says more than 500 cases of the new coronavirus stemmed from prisons. (2020). Available at: <https://www.cnbc.com/2020/02/21/coronavirus-china-says-two-prisons-reported-nearly-250-cases.html>. (Accessed: 25th March 2020)
26. Chong, K. C. et al. Affiliations : *medRxiv* (2020).
27. Sina News. Wuhan lockdown. (2020). Available at: <https://news.sina.com.cn/c/2020-02-15/doc-iimxxstf1526561.shtml>. (Accessed: 10th March 2020)
28. NY Post. Italy's coronavirus lockdown extended to entire country. (2020). Available at: <https://nypost.com/2020/03/09/italys-coronavirus-lockdown-extended-to-entire-country>. (Accessed: 25th March 2020)
29. Guardian. South Korea took rapid, intrusive measures against Covid-19 – and they worked. Available at: <https://www.theguardian.com/commentisfree/2020/mar/20/south-korea-rapid-intrusive-measures-covid-19>. (Accessed: 20th March 2020)
30. Observers. Food, water and masks: South Korea's COVID-19 quarantine kits. (2020).

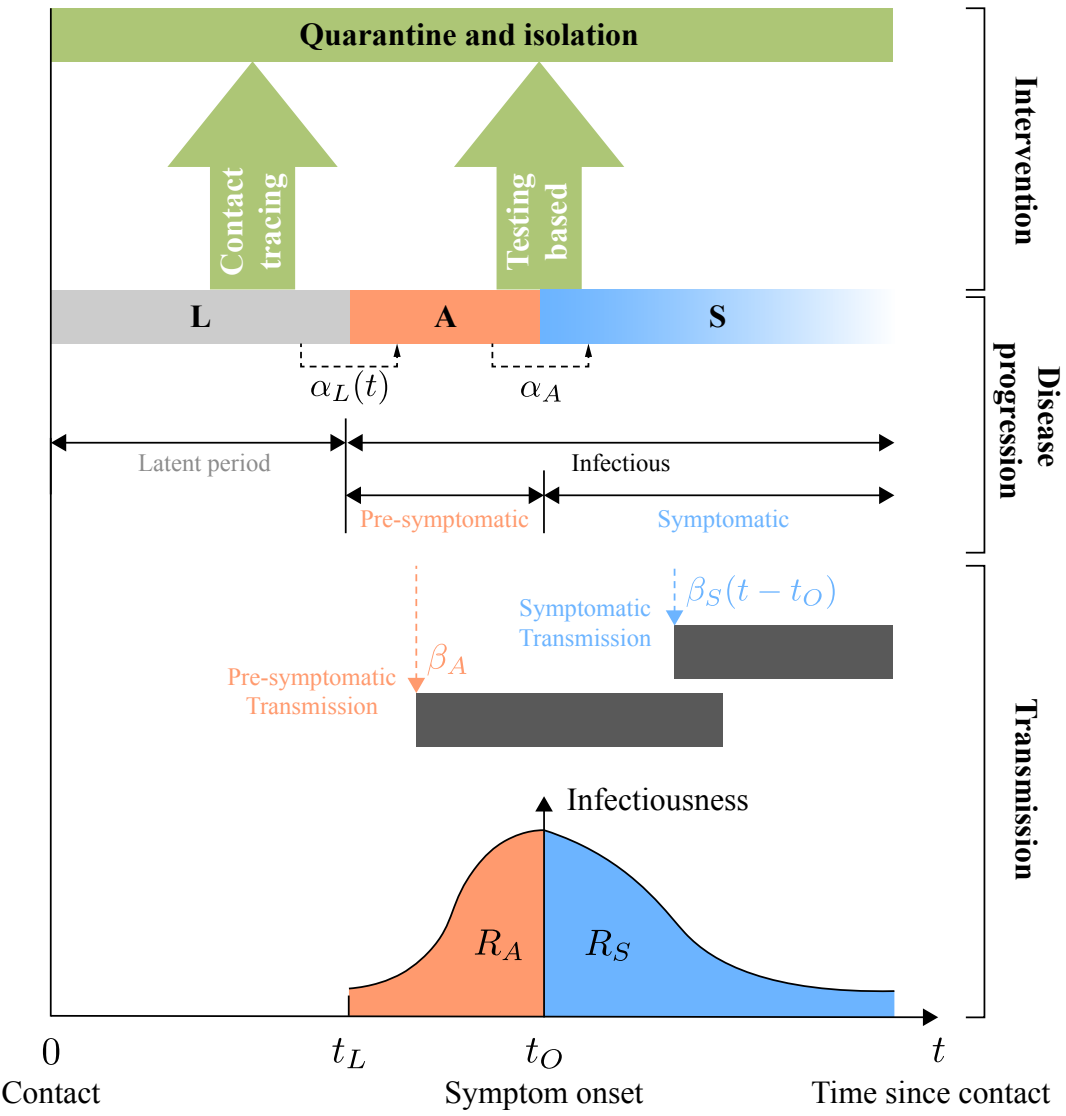


**Figure 1. Transmission of COVID-19 during disease progression and intervention.** COVID-19 disease progression and transmission: A person infected at time  $t = 0$  first goes through a non-infectious latent phase (L) until  $t_L$ , marking the start of the infectious period. The infectious period consists of two phases, pre-symptomatic (A) and symptomatic (S). In phase A, the person is infectious without symptoms, during which the virus can be spread through pre-symptomatic transmission (orange dashed arrow). At the symptom onset time  $t_O$ , the person enters the S phase and infects others with symptomatic transmission (blue dashed arrow). The infectiousness of the person peaks around the symptom onset time. The basic reproduction number  $R_0$  is split into  $R_A$  and  $R_S$ , given by areas underneath the curve on either side of the symptom onset point, respectively. Interventions to limit transmission: contact tracing brings an infected person out of the transmission cycle at the point of isolation, while testing is effective only when the person has developed high viral load and is already in the infectious period.

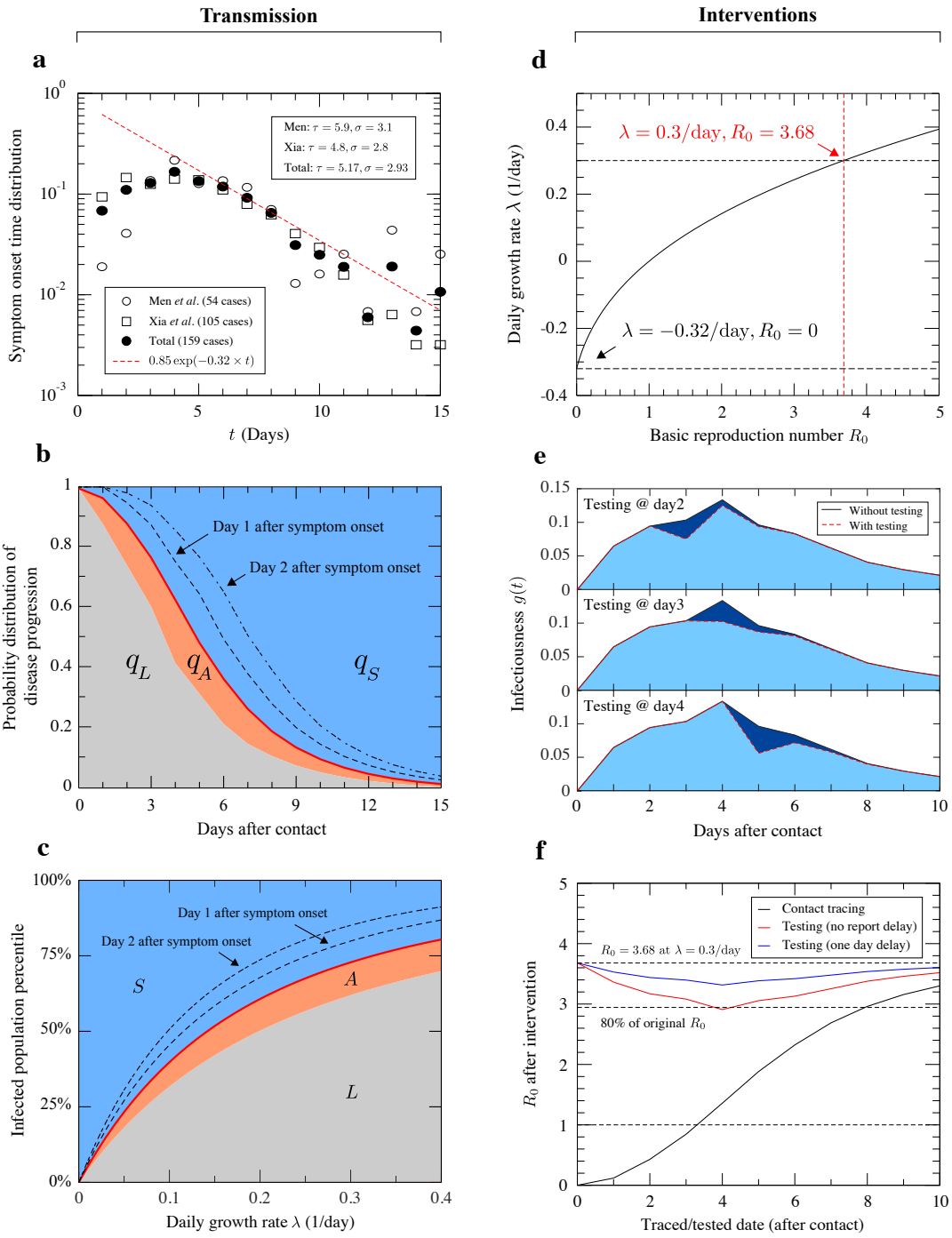


**Figure 2. Data and model predictions.** **a**, The symptom onset time distribution. Two data sets from previous studies are shown (hollow circles<sup>32</sup> and squares<sup>15</sup>). The mean values and standard deviations are given in the legend. The distribution of the union of the two datasets is shown in solid circles. The red dashed line gives a reference exponential function shown in the legend. **b**, Probabilities for an infected individual being in each of the three phases at day  $t$  after infection. The red curve indicates the boundary between the L+A and S phases. The probabilities that an individual is one day or two days into the S phase can be obtained from respective areas bounded by

dashed and dashed-dotted curves, respectively. **c**, Percentage of the infected population in each phase when the epidemic is growing at a rate  $\lambda$ . The red curve indicates the boundary between the L+A and S phases. The percentages of the population one day or two days into the S phase are indicated by dashed and dashed-dotted lines, respectively. **d**, The relationship between the growth rate  $\lambda$  and basic reproduction number  $R_0$ . At  $\lambda = 0.3$ ,  $R_0$  is 3.68. **e**, Reproduction rate  $r(t)$  (arbitrary units) from our model (black lines) and its revised values under one-time testing (red dashed lines) performed on day 2 (top), day 3 (middle) and day 4 (bottom) after contact. The basic reproduction number  $R_0$  is given by the area under the curve in each case. **f**, Reduction of basic reproduction number  $R_0$  against intervention time, calculated from the day of infection. Results are given for contact tracing and isolation (black line) and testing with 0 or 1 day reporting delay (red, blue curves). The value of  $R_0$  at 3.68 corresponds to a growth rate  $\lambda = 0.3$ . Time is measured in days.

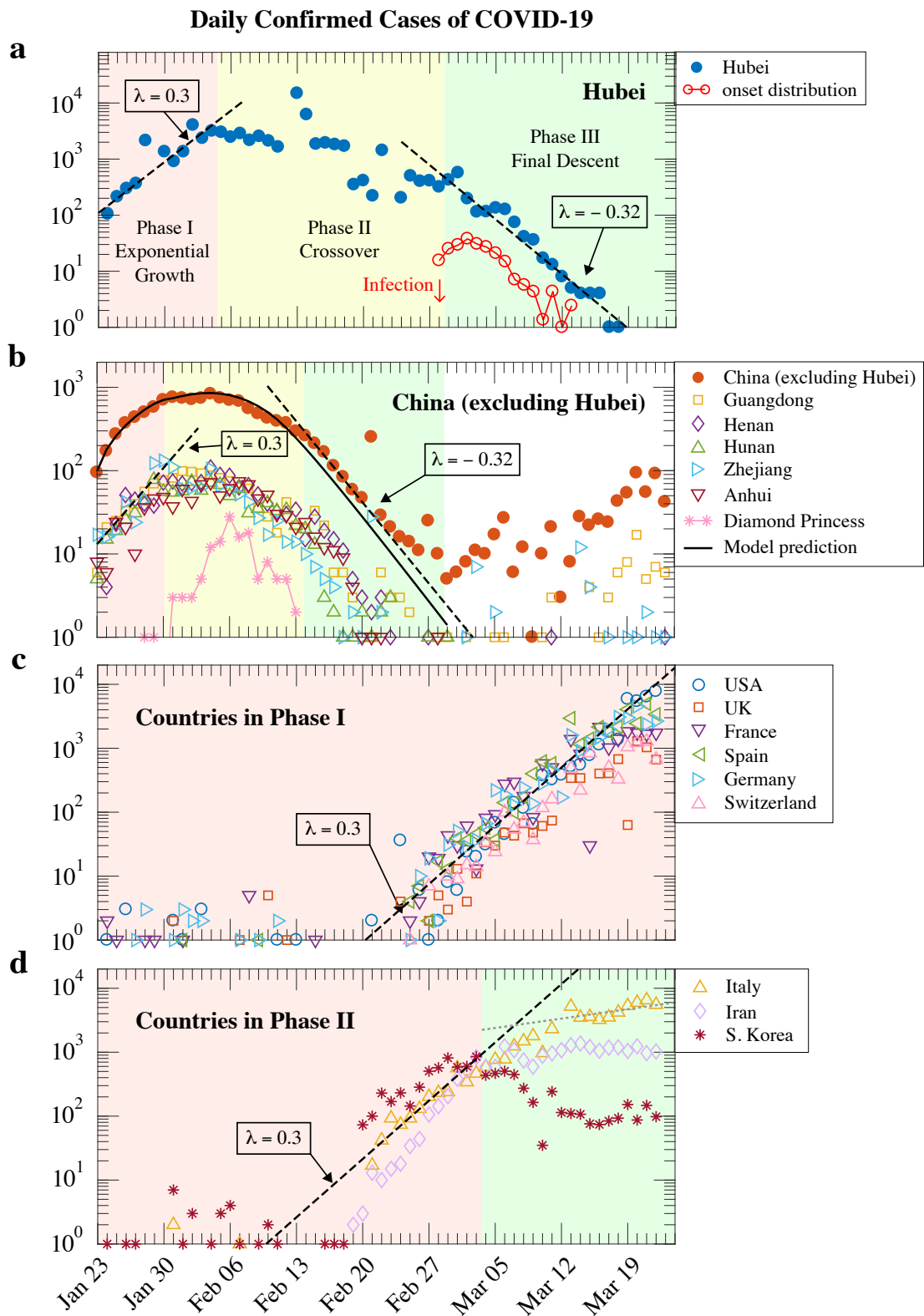


**Figure 3. The COVID-19 epidemic development in various countries and regions.** Daily confirmed cases in China and other affected countries since the Wuhan lockdown on January 23, 2020. **a**, Hubei province. The three phases of the epidemic development are marked in color: exponential growth (red), crossover (yellow), and

descent phase (green). Early exponential growth reached a rate  $\lambda$  at approximately 0.3/day (left dashed line). Growth slowed and entered the crossover phase in the middle of the second week, and reached the third phase nearly four weeks later. The final descent that began in the beginning of March is characterised by  $\lambda = -0.32/\text{day}$  (right dashed line). The incubation period distribution is shown in red circles to compare with the exponential decay. **b**, China (excluding Hubei province). The epidemic development in the main affected provinces followed a nearly identical three-phase pattern. Also shown is the model-predicted evolution of the number of daily confirmed cases (solid line), with details given in Supplementary Information. The increase in the number of newly confirmed cases since the beginning of March is due to imported cases (white region). Data for the Diamond Princess cruise ship is included for comparison. **c**, Countries in phase I. The epidemic progress in these countries is still in the exponential growth phase with a daily rate  $\lambda$  of around 0.3 (dashed line). **d**, Countries entering or in the middle of phase II. South Korea has reached zero growth in daily confirmed cases, while data from Iran and Italy indicate a slowing down of the exponential growth. After the national quarantine on March 9, the growth in Italy slowed down with a rate of around 0.05/day (gray dotted line).

## Supplementary Information

### Quantifying the Infected Population for Calibrated Intervention and Containment of the COVID-19 Pandemic

In this Supplementary Information, a stochastic model of the infected population in a given communal outbreak is constructed and analysed. The model is set up around the population dynamics of pre-symptomatic carriers. The size of the other infected groups can be inferred through simple mathematical equations.

#### I. The Mathematical Model

##### The governing equation

The basic structure of our model follows Fig. 1 in the Main Text, with model parameters defined in Fig. S1. The disease progression parameters  $\alpha_A$  and  $\alpha_L(t_L)$  are taken to be universal, while the transmission rates  $\beta_A$  and  $\beta_s(t_s)$  may vary significantly from community to community.

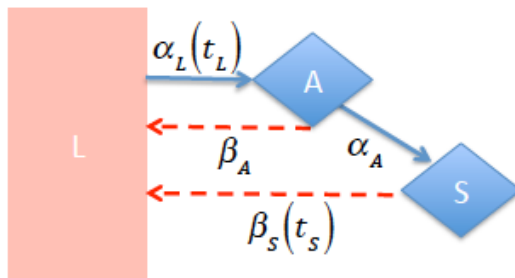


**Figure S1. A stochastic model for disease progression and transmission.** Disease progression of an infected individual is assumed to be described by a renewal process following the sequence of latent (L), pre-symptomatic (A) and symptomatic (S) phases. The transition rate from L to A is given by  $\alpha_L(t_L)$  and depends on the duration  $t_L$  of the latent phase. Transition from A to S is Poisson at a constant rate  $\alpha_A$ . Both A and S are infectious, with

transmission rates to reproduce secondary cases at  $\beta_A$  and  $\beta_S(t_S)$ , respectively. The latter is a function of  $t_S$ , the number of days since symptom onset.

We now consider the groups of infected individuals in L, A and S in a large population, using the same symbol to denote their size. The generation rate of L at time  $t$  is given by,

$$J_L(t) = \beta_A A(t) + \int_{-\infty}^t \beta_S(t-t_2) dS(t_2)$$

Those “newly infected” eventually make their way to A. The flux to A due to a group infected at a time  $t_1 < t$  is given by,

$$dJ_A(t) = \alpha_L(t-t_1) q_L(t-t_1) J_L(t_1) dt_1$$

where

$$q_L(t) = e^{-\int_0^t \alpha_L(t_1) dt_1}$$

is the probability that an individual infected at  $t=0$  remains in the latent phase L. Adding up contributions from all such groups, we obtain

$$J_A(t) = \int_{-\infty}^t \alpha_L(t-t_1) q_L(t-t_1) J_L(t_1) dt_1$$

Note that in our model,  $dS(t) = \alpha_A A(t) dt$ , we have then

$$\begin{aligned} J_A(t) &= \int_{-\infty}^t \beta_A \alpha_L(t-t_1) q_L(t-t_1) A(t_1) dt_1 + \int_{-\infty}^t \alpha_L(t-t_1) q_L(t-t_1) dt_1 \int_{-\infty}^{t_1} \beta_S(t_1-t_2) \alpha_A A(t_2) dt_2 \\ &= \int_{-\infty}^t K(t-t_1) A(t_1) dt_1 \end{aligned}$$

Here the kernel function is given by,

$$K(t) = \beta_A \alpha_L(t) q_L(t) + \alpha_A \int_0^t \alpha_L(t-t_1) q_L(t-t_1) \beta_S(t_1) dt_1 \quad (S1)$$

The final equation for A takes the form,

$$\dot{A} = -\alpha_A A + \int_{-\infty}^t K(t-t_1) A(t_1) dt_1 \quad (S2)$$

### Kernel function from observed symptom onset time distribution

As we show below, a major advantage of our model is that the kernel function in Eq. (S2) can be determined from the statistics of the time interval between infection and symptom onset

$\tau_o = \tau_L + \tau_A$ , directly observable from clinical case studies. Denoting by  $p_o(t)$  the probability distribution function of  $\tau_o$ . The probabilities for an individual infected at  $t=0$  to be in one of the three phases are given in Table S1.

**Table S1.** Probabilities an individual infected at  $t=0$  is in each of the disease phases at time  $t$ .

Phase	Probability	Expression
Latent	$q_L(t)$	$1 - \alpha_A^{-1} p_o(t) - \int_0^t p_o(t_1) dt_1$
Pre-symptomatic Infectious w/o symptom	$q_A(t)$	$\alpha_A^{-1} p_o(t)$
Symptomatic	$q_S(t)$	$\int_0^t p_o(t_1) dt_1$

In terms of Laplace transforms defined by  $\tilde{f}(\lambda) = \int_0^\infty f(t) e^{-\lambda t} dt$ , we have

$$\tilde{q}_L(\lambda) = \frac{1}{\lambda} - \left( \frac{1}{\alpha_A} + \frac{1}{\lambda} \right) \tilde{p}_o(\lambda) \quad (\text{S3})$$

The Laplace transform of Eq. (S1) takes the form,

$$\tilde{K}(\lambda) \equiv \int_0^\infty K(t) e^{-\lambda t} dt = [\beta_A + \alpha_A \tilde{\beta}_S(\lambda)] [1 - \lambda \tilde{q}_L(\lambda)]$$

With the help of (S3), we obtain

$$\tilde{K}(\lambda) = [\beta_A + \alpha_A \tilde{\beta}_S(\lambda)] \left( 1 + \frac{\lambda}{\alpha_A} \right) \tilde{p}_o(\lambda) \quad (\text{S4})$$

Hence the dynamics of the disease transmission can be formulated in terms of the symptom onset time distribution.

### Mean reproduction rate and $R_0$

Equation (S2) can be alternatively formulated in terms of the mean reproduction rate  $r(t)$  of an individual infected at  $t=0$ . In our current setting,

$$\begin{aligned}
r(t) &= \beta_A \int_0^t q_L(t_1) \alpha_L(t_1) dt_1 e^{-\alpha_A(t-t_1)} + \int_0^t q_L(t_1) \alpha_L(t_1) dt_1 \int_{t_1}^t \beta_S(t-t_2) \alpha_A dt_2 e^{-\alpha_A(t_2-t_1)} \\
&= \int_0^t dt_1 K(t_1) e^{-\alpha_A(t-t_1)}
\end{aligned} \tag{S5}$$

where the last step is written by comparing with the expression for  $J_A(t)$ .

The basic reproduction number is given by

$$R_0 = \int_0^\infty r(t) dt = \int_0^\infty \beta_A t e^{-\alpha_A t} \alpha_A dt + \int_0^\infty \beta_S(t) dt = \frac{\beta_{\text{eff}}}{\alpha_A} \tag{S6}$$

Here

$$\beta_{\text{eff}} = \beta_A + \alpha_A \tilde{\beta}_S(0) \tag{S7}$$

is a key model parameter that sets the overall transmission speed of our model.

### Exponential growth/decay

The self-sustained growth rate  $\lambda$  of an outbreak can be obtained by seeking a solution

$A(t) = e^{\lambda t}$  to Eq. (S2). Simple algebra gives

$$\lambda = -\alpha_A + \tilde{K}(\lambda) \tag{S8}$$

Combining Eqs. (S4) with Eq. (S8), we obtain,

$$[\beta_A + \alpha_A \tilde{\beta}_S(\lambda)] \left( 1 + \frac{\lambda}{\alpha_A} \right) \tilde{p}_o(\lambda) = \lambda + \alpha_A$$

or

$$[\beta_A + \alpha_A \tilde{\beta}_S(\lambda)] \tilde{p}_o(\lambda) = \alpha_A \tag{S9}$$

In the epidemiological literature, it is customary to express the growth rate  $\lambda$  in terms of  $R_0$ .

From Eqs. (S6) and (S9), we obtain,

$$R_0 = \frac{1}{\tilde{p}_o(\lambda)} \frac{\beta_A + \alpha_A \tilde{\beta}_S(0)}{\beta_A + \alpha_A \tilde{\beta}_S(\lambda)} \tag{S10}$$

At  $\lambda = 0$ ,  $R_0 = 1$  as required, independent of the model parameters.

Equation (S10) expresses the fundamental mechanism for epidemic growth, i.e., the basic reproduction number of infected individuals drives the growth rate of the epidemic. The Laplace transform of the symptom onset time plays a pivotal role in our model. One immediate result from Eq. (S10) is that  $R_0 = 0$  is at the pole of  $\tilde{p}_o(\lambda)$ . For  $p_o(t) \sim e^{-\lambda_0 t}$ , the pole is at  $\lambda = -\lambda_0$ , which yields the rate of decay when transmission stops completely.

### Generation time interval

Walling and Lipsitch [1] proposed a general equation between  $R_0$  and  $\lambda$  based on the normalized “generation interval distribution”,

$$g(t) = r(t)/R_0 \quad (\text{S11})$$

At the observed population growth rate  $\lambda$ , each individual produces  $R_0(\lambda)$  offspring.

Consequently,

$$\tilde{g}(\lambda) = \frac{\tilde{r}(\lambda)}{R_0} = \frac{1}{R_0}$$

known as the Lotka–Euler estimating equation. This equation is equivalent to (S10).

### Percentage of subpopulations during exponential growth

Let  $J_L(t) = J_L(0)e^{\lambda t}$  be the flux of newly infected individuals. The population size in each phase can be expressed as Laplace transforms of expressions in Table S1,

$$\begin{aligned} L(t) &= \int_{-\infty}^t q_L(t-t_1) J_L(t_1) dt_1 = \left[ \frac{1}{\lambda} - \left( \frac{1}{\alpha_A} + \frac{1}{\lambda} \right) \tilde{p}_o(\lambda) \right] J_L(t) \\ A(t) &= \int_{-\infty}^t q_A(t-t_1) J_L(t_1) dt_1 = \frac{1}{\alpha_A} \tilde{p}_o(\lambda) J_L(t) \\ S(t) &= \int_{-\infty}^t q_S(t-t_1) J_L(t_1) dt_1 = \frac{1}{\lambda} \tilde{p}_o(\lambda) J_L(t) \end{aligned} \quad (\text{S12})$$

For easy reference, the percentages of subpopulations are collected in Table S2.

**Table S2.** Percentage of the infected in each group when the whole population grows at a rate  $\lambda$ .

Phase	Percentage	Expression
Latent	$Q_L(\lambda)$	$1 - \tilde{p}_o(\lambda) - \frac{\lambda}{\alpha_A} \tilde{p}_o(\lambda)$
Pre-symptomatic Infectious w/o symptom	$Q_A(\lambda)$	$\frac{\lambda}{\alpha_A} \tilde{p}_o(\lambda)$
Symptomatic	$Q_S(\lambda)$	$\tilde{p}_o(\lambda)$

## II. Simplifying Approximations

The expressions above that relate various quantities to  $p_o(t)$  are mostly expressed in Laplace transforms, which are inconvenient to use. Here we consider simplifying approximations which are more handy when it comes to making analytical predictions.

### Mapping symptom onset time distribution to generation time interval distribution

Under good self-quarantine practice, or when the public health and medical resources are not overstretched, symptomatic transmission is limited to the first one or two days after symptom onset. In such a scenario,  $\tilde{\beta}_s(\lambda)$  has a weak dependence on  $\lambda$ ,

$$\tilde{\beta}_s(\lambda) = \int_0^\infty \beta_s(t) e^{-\lambda t} dt \approx \tilde{\beta}_s(0)(1 - \lambda \tau_s) \quad (\text{S13})$$

where  $\tilde{\beta}_s(0)$  is the area underneath the infectiousness curve on the symptomatic side of Fig. 1, in the Main Text, and

$$\tau_s = \tilde{\beta}_s^{-1}(0) \int_0^\infty t \beta_s(t) dt$$

is the width of the curve on the symptomatic side. Substituting (S13) into (S4), we obtain,

$$\tilde{K}(\lambda) = \beta_{\text{eff}} \left( 1 + \frac{\lambda}{\alpha_A} \right) \tilde{p}_{o,\text{eff}}(\lambda) \quad (\text{S14})$$

where

$$\tilde{p}_{o,\text{eff}}(\lambda) = (1 - \tau_{\text{eff}} \lambda) \tilde{p}_o(\lambda) \quad (\text{S15})$$

with

$$\tau_{\text{eff}} = \tau_s \left( 1 - \frac{\beta_A}{\beta_{\text{eff}}} \right)$$

Under this re-parameterisation, the integration kernel takes the explicit form,

$$K(t) = \beta_{\text{eff}} \left[ p_{o,\text{eff}}(t) + \alpha_A^{-1} \frac{d}{dt} p_{o,\text{eff}}(t) \right] \quad (\text{S16})$$

From Eq. (S5), we obtain a very simple expression for the reproduction rate,

$$r(t) = R_0 p_{o,\text{eff}}(t) \quad (\text{S17})$$

Hence,  $p_{0,\text{eff}}(t)$  is nothing but the generation time interval distribution  $g(t)$ .

A few remarks with regard to the re-parameterised model are in order. As explained in the Main Text,  $\beta_{\text{eff}}$  incorporates contributions from both pre-symptomatic and symptomatic individuals (Fig. 1, Main Text). The mean value of the symptom onset time from the re-parameterised distribution is given by

$$\langle t_o \rangle_{\text{eff}} = -\tilde{p}_{0,\text{eff}}'(0) = \tau_{\text{eff}} + \tau_o$$

where  $\tau_o$  is the mean of the symptom onset time distribution in the original model. This is due to the incorporation of transmission by symptomatic patients.

**Important Note:** In the more general case, a model based on Eq. (S4) can be mapped to an effective model given by Eq. (S14) with a symptom onset time distribution given by the generation time interval  $g(t)$  whose Laplace transform is obtained from the data  $\tilde{p}_o(\lambda)$ ,

$$\tilde{g}(\lambda) = \frac{\tilde{r}(\lambda)}{R_0} = \frac{\beta_A + \alpha_A \tilde{\beta}_S(\lambda)}{\beta_{\text{eff}}} \tilde{p}_o(\lambda) \quad (\text{S18})$$

In this effective model, an infected individual is infectious only in phase A, which may cause certain confusion when not explained properly. Nevertheless, it is mathematically fully equivalent to the original model in terms of Eq. (S2) for the epidemic dynamics that takes care of transmission by both pre-symptomatic and symptomatic viral carriers.

### A Markovian model

A number of modeling studies in the literature adopt a Markovian set up with  $\alpha_L(t) = \text{const.}$  which is a special case of our more general non-Markovian approach. In particular,

$$\tilde{q}_L = \frac{1}{\alpha_L + \lambda}, \quad \tilde{p}_o = \frac{\alpha_L}{\alpha_L + \lambda} \frac{\alpha_A}{\alpha_A + \lambda} \quad (\text{S19})$$

The onset time distribution in this case is given by

$$p_o(t) = \frac{\alpha_L \alpha_A}{\alpha_A - \alpha_L} \left[ e^{-\alpha_L t} - e^{-\alpha_A t} \right] = \frac{1}{\tau_L - \tau_A} \left( e^{-t/\tau_L} - e^{-t/\tau_A} \right)$$

with its mean and variance given by,

$$\tau_o = \langle t_o \rangle = \tau_L + \tau_A, \quad \sigma_o^2 = \langle t_o^2 \rangle - \langle t_o \rangle^2 = \tau_L^2 + \tau_A^2, \quad \frac{\sigma_o^2}{\tau_o^2} = \varepsilon^2 + (1 - \varepsilon)^2$$

where  $\tau_L = \varepsilon \tau_o$ ,  $\tau_A = (1 - \varepsilon) \tau_o$ . In the limit  $\tau_L = \tau_A$  or  $\varepsilon = 1/2$ ,  $p_o(t) = \frac{t}{\tau_L^2} e^{-t/\tau_L}$ .

The Laplace transform of the kernel function then takes the form,

$$\tilde{K}_M(\lambda) = \alpha_L \frac{\beta_A + \alpha_A \tilde{\beta}_S(\lambda)}{\alpha_L + \lambda} \simeq \alpha_L \frac{\beta_{\text{eff}} (1 - \tau_{\text{eff}} \lambda)}{\alpha_L + \lambda} \simeq \alpha_{L,\text{eff}} \frac{\beta_{\text{eff}}}{\alpha_{L,\text{eff}} + \lambda}$$

where  $\alpha_{L,\text{eff}} = \alpha_L / (1 + \alpha_L \tau_{\text{eff}})$  gives the reduced effective rate to exit the latent phase, in agreement with (S16). Performing the inverse transform yields

$$K_M(t) \simeq \beta_{\text{eff}} \alpha_{L,\text{eff}} e^{-\alpha_{L,\text{eff}} t} \quad (\text{S20})$$

Let  $\tau_o = \alpha_{L,\text{eff}}^{-1} + \alpha_A^{-1}$ ,  $\varepsilon = \frac{\alpha_A}{\alpha_{L,\text{eff}} + \alpha_A}$ , we have,

$$R_0 \simeq \left( 1 + \frac{\lambda}{\alpha_{L,\text{eff}}} \right) \left( 1 + \frac{\lambda}{\alpha_A} \right),$$

i.e., a parabola with two nodes at  $\lambda_L \simeq -\alpha_{L,\text{eff}}$  and  $\lambda_A \simeq -\alpha_A$ .

### III. Calibration of Model Parameters

#### Symptom onset time distribution from case studies

The incubation periods of individual patients before symptom onset were summarized in 2 preprints: 54 cases collected by Men et al.[2], and 105 cases collected by Xia et al.[3]. In total, we examined 159 cases with their incubation periods. For cases when the initial contact can only be assigned to a time interval spanning more than one day, we simply assume equal probability for each day inside the interval. We then include all case counts to construct the histogram of symptom onset time, rendering the result shown in Fig. 2a of the Main Text. The mean onset time is 5.17 days, with a standard deviation of 2.93 days. The tail of the distribution can be well-fitted to an exponential decay function with a rate of  $-0.32/\text{day}$ .

#### Serial interval statistics

Du et al. [4] reported the statistics of the time lag in symptom onset between infector–infectee pairs in 468 confirmed serial infection cases, which we use to check against the symptom onset distribution function obtained above.

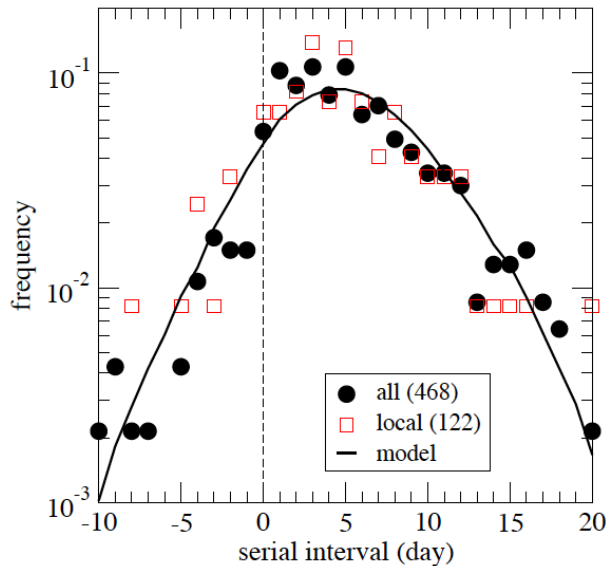


**Figure S2. Predicted serial interval distribution vs. real data.** The data collected by Du et al. [4] on the serial interval distribution is shown in black dots (all 468 pairs) and red squares (122 local infections). The solid line is our model prediction using the data for the incubation period as input. See text for details.

Let  $t = 0$  be the time point when the infector X contracted the virus, the distribution of the transmission time  $t_{x \rightarrow y}$  from X to Y is  $g(t)$ .

We now consider the distribution of the difference in symptom onset time  $t_{xy} = t_y - t_x$  between X and Y. The distribution of  $t_x$  is given by  $p_o(t)$ . The distribution of  $t_y = t_{x \rightarrow y} + t_x$  can also be expressed as a convolution of  $g(t)$  and  $p_o(t)$ . According to Eq. (S10),  $g(t) \approx p_o(t)$  when symptomatic transmission is limited to around the symptom onset time. In

this case, all three quantities have the same distribution. Consequently,  $\sigma_x = \frac{\sigma_{xy}}{\sqrt{3}}$ .

From the Table S1 of Ref [2], we get SD value 2.74 days, in good agreement with the value 2.93 days from our analysis. Close examination of the data shows a discontinuity across the origin, which may be attributed to the false assignment of infector and infectee in a pair. As noted by Du et al.<sup>4</sup>, cluster infections (such as intra-family transmission) could also yield a lower value for the serial interval on average, contributing to the discrepancy seen in the figure. Overall, the comparison lends strong support for the aggregated symptom onset time distribution obtained, as well as for our model assumptions.

#### Infectiousness around symptom onset and $\alpha_A$

Xia et al. [3] documented the infection date of 74 secondary cases in relation to the symptom onset date of the first generation. Data for the number of transmissions against days after symptom onset are replotted in Fig. S3 with solid circles, ranging from 5 days before to 8 days after. Only 27% of the cases fall on or after the symptom onset date, while peak transmission happens two days before under the definition of symptoms adopted. The cumulative number of cases are shown by open circles. The left tail can be fitted to an exponential function with a decay rate in the range  $\alpha_A = 0.7/\text{day}$  to  $0.82/\text{day}$ . A value  $\alpha_A = 0.75/\text{day}$  is used in our numerical explorations. As seen in Tables S1 and S2, this parameter affects the size of the infectious A subpopulation. Since the actual reproduction rate is controlled by  $R_0 = \beta_{\text{eff}} / \alpha_A$ , the actual value of  $\alpha_A$  is not important when the data is interpreted correctly. The outliers on

the far right are not of concern in this work, as they are likely to be quarantined given the heightened attention on COVID-19.

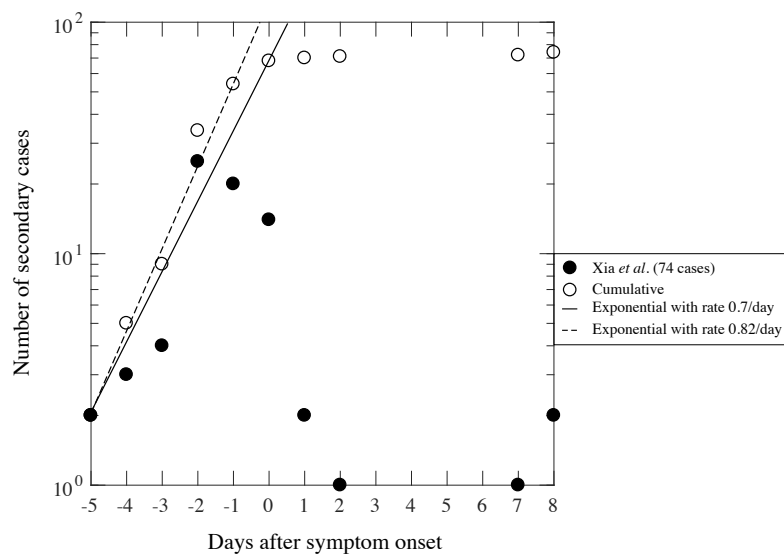


**Figure S3. The number of secondary cases against the symptom onset date of the first generation cases.** Data from Xia et al.[3]

## IV. Model Exploration under Intervention

### Testing and quarantining

Testing and quarantining of infected individuals is practiced in South Korea with great intensity. In the simplest scenario, a suspected individual undergoes testing of the COVID-19 infection. It takes a day or so for the test result to come back. If it is positive, the person will be quarantined and hence removed from the active infected population. Oral tests for the virus reports only cases with sufficiently high viral load. Therefore the test needs to be done around the time of symptom onset. However, by then the person may have already infected other people. Within our probabilistic framework, the efficiency of this procedure can be assessed from the reduction of the reproduction rate  $r(t)$ ,

Adopting the simplified model (S17), we can write, under testing,

$$r_{\text{testing}}(t) = r(t) - \beta_{\text{eff}} \int_0^t dt_1 \eta_{\text{testing}}(t_1) q_A(t_1) e^{-\alpha_A(t-t_1-\tau_d)} \quad (\text{S21})$$

Here  $\eta_{\text{testing}}(t)$  is the test protocol that gives the rate of testing per individual on day  $t$  since infection, and  $\tau_d$  is the delay in producing the report. To maximise reduction, the test time should be chosen to be around the peak of the product

$$q_A(t) \approx \alpha_A^{-1} p_0(t)$$

which is around 4 days after contact.

In the extreme case of testing at a particular time point day  $T$  with no test delay, we have

$$r_{\text{testing}}(t) = \begin{cases} r(t), & t < T \\ r(t) - q_T \alpha_A R_0 q_A(T) e^{-\alpha_A(t-T-\tau_a)}, & t > T \end{cases} \quad (\text{S22})$$

Here  $q_T$  is the percentage of close contacts of infected individuals being tested. Integrating the equation over time yields the reduction in  $R_0$ ,

$$\Delta R_0 = -R_0 q_A(T) e^{-\alpha_A \tau_a} \quad (\text{S23})$$

The expression for  $q_A(T)$  can be found in Table S1.

### Contact tracing

In contact tracing, all close contacts of a newly confirmed viral carrier are identified and quarantined soon after the contact took place, without testing. This procedure is more effective as it also covers those infected but still in the latent phase of their disease development. Thus  $r(t)$  is truncated on the day the contact is found, while the person could still be transmitting the disease before that time. The reduction of  $R_0$  in this case is given by,

$$\Delta R_0 = -q_c \int_T^\infty r(t) dt = -q_c R_0 [1 - q_s(T)]$$

Here  $q_c$  is the probability to reach the contact. Expression for  $q_s(T)$  is given in Table S1.

### Solution with imported cases

Border control measures can effectively stop imported cases of viral carriers. To examine the time needed for their effect to take place, let us first consider growth driven by imported cases when unchecked. Under a daily flux  $J_{\text{ext}}(t)$  of imported cases, Eq. (S2) is modified to,

$$\dot{A} = -\alpha_A A + \int_{-\infty}^t K(t-t_1) A(t_1) dt_1 + J_{\text{ext}}(t) \quad (\text{S24})$$

Consider a simple situation where the imported cases grow exponentially with a rate  $\lambda_I$ , i.e.,

$J_{\text{ext}}(t) = J_I e^{\lambda_I t}$ . Let's seek an exponentially growing solution where the local population is driven by the imported cases,

$$\begin{aligned} A(t) &= A_{\text{all}} e^{\lambda_I t} \\ (\lambda_I + \alpha_A) A_{\text{all}} &= A_{\text{all}} \tilde{K}(\lambda_I) + J_I \\ A_{\text{all}} &= \frac{J_I}{\lambda_I + \alpha_A - \tilde{K}(\lambda_I)} \end{aligned}$$

The fraction of local infections after the initial transient is given by,

$$\frac{A_{\text{local}}}{A_{\text{all}}} = \frac{\tilde{K}(\lambda_I)}{\lambda_I + \alpha_A} \quad (\text{S25})$$

In many cases, the ratio of imported and local infections is known. Equation (S25) can then be used to calibrate the level of local transmission when the imported cases grow exponentially at a rate greater than the one given in Table S2 for local outbreak.

We consider here a situation where the disease transmission rate per infected individual in a given community gradually weakens according to the schedule,

$$\eta(t) = 1 - (1 - \eta_1) \frac{t - t_0}{T}, \quad t_0 < t < t_0 + T$$

Here  $t_0$  is the starting date and  $T$  is the duration of the change. After this period,  $\eta(t) = \eta_1$ .

Equation (S2) then takes the form,

$$\dot{A} = -\alpha_A A + \int_{-\infty}^t K(t - t_1) \eta(t_1) A(t_1) dt_1 \quad (\text{S26})$$

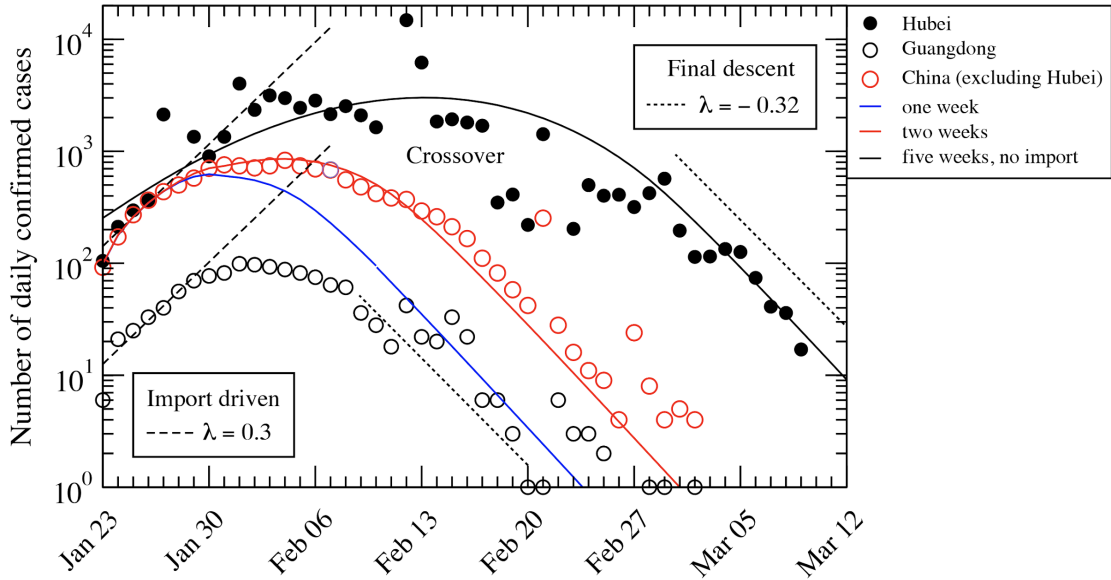


**Figure S4. Simulation of the number of daily confirmed cases with a linear decay of transmission per infected individual.** The number of daily confirmed cases in Hubei, Guangdong and China (excluding Hubei) are replotted for comparison. Cluster infections result in occasional bursts in the time series which are not modelled in this work.

We used Eq. S(26) to simulate the bell-shaped epidemic development curves in China after the Wuhan lockdown (Figs. 3a and 3b, Main Text), taking  $\eta_1 = 0$ . The starting time of the social distancing policy  $t_0$  is chosen to be one week after the lockdown. The blue, red and black curves in Fig. S4 correspond to three different values of  $T$  given in the legend. The situation

represented by blue and red curves is initially driven by imported cases whose number grows exponentially at a rate  $\lambda_0 = 0.2$  prior to the lockdown, with an amplitude that decreases linearly and vanishes on the 10th day after the lockdown. No imported cases were introduced to generate the black curve. Taken at face value, our model can reproduce fast or slow crossovers seen in the data from various provinces of China. Further discussion can be found in the Main Text.

### House confinement

The situation on the cruise ship Diamond Princess is close to a sudden complete confinement of the passengers. Such a scenario is described by the schedule function

$$\eta(t) = \begin{cases} 1, & t < t_0 \\ \eta_1, & t > t_0 \end{cases}$$

at  $\eta_1 = 0$ . Under the Markovian assumption introduced above, the change over from exponential growth to exponential decay can be solved analytically.

Without loss of generality, we may define our time such that  $t_0 = 0$ . Take  $A(t) = A_0 e^{\lambda_0 t}$  for  $t < t_0 = 0$ , we may rewrite Eq. (S26) as,

$$\dot{A} = -\alpha_A A + \beta_0 \int_{-\infty}^0 \alpha_L(t-t_1) q_L(t-t_1) A_0 e^{\lambda_0 t_1} dt_1 + \beta_1 \int_0^t \alpha_L(t-t_1) q_L(t-t_1) A(t_1) dt_1$$

Taking the Laplace transform, we have,

$$-A_0 + \lambda \tilde{A}(\lambda) = -\alpha_A \tilde{A}(\lambda) + \tilde{K}_1(\lambda) \tilde{A}(\lambda) + \tilde{S}(\lambda)$$

which yields

$$\tilde{A}(\lambda) = \frac{\tilde{S}(\lambda) + A_0}{\alpha_A + \lambda - \tilde{K}_1(\lambda)} \quad (\text{S27})$$

Here

$$\begin{aligned} S(t) &= \beta_0 A_0 \int_{-\infty}^0 \alpha_L(t-t_1) q_L(t-t_1) e^{\lambda_0 t_1} dt_1 \\ &= \beta_0 A_0 \int_{-\infty}^t \alpha_L(t-t_1) q_L(t-t_1) e^{\lambda_0 t_1} dt_1 - \beta_0 A_0 \int_0^t \alpha_L(t-t_1) q_L(t-t_1) e^{\lambda_0 t_1} dt_1 \\ \tilde{S}(\lambda) &= \beta_0 A_0 \frac{\widetilde{\alpha_L q_L}(\lambda_0) - \widetilde{\alpha_L q_L}(\lambda_0)}{\lambda - \lambda_0} = \beta_0 A_0 \frac{\lambda \tilde{q}_L(\lambda) - \lambda_0 \tilde{q}_L(\lambda_0)}{\lambda - \lambda_0} \end{aligned}$$

Under the Markovian assumption (S18), we have  $\tilde{q}_L(\lambda) = \frac{1}{\alpha_L + \lambda}$

$$\begin{aligned}\tilde{S}(\lambda) &= \beta_0 A_0 \frac{\lambda(\alpha_L + \lambda_0) - \lambda_0(\alpha_L + \lambda)}{\lambda - \lambda_0} \frac{1}{(\alpha_L + \lambda_0)(\alpha_L + \lambda)} \\ &= \frac{\alpha_L \beta_0 A_0}{\alpha_L + \lambda_0} \frac{1}{\alpha_L + \lambda}\end{aligned}$$

The kernel function under the new policy is given by

$$\tilde{K}_1(\lambda) = \frac{\alpha_L}{\alpha_L + \lambda} \beta_1$$

Carrying out inverse transform of Eq. (S23) yields

$$A(t) = (\lambda_0 + \alpha_A + \gamma_A) A_0 (A_+ e^{\lambda_+ t} + A_- e^{\lambda_- t} + A_1 e^{-\alpha_L t}) + A_0 (B_+ e^{\lambda_+ t} + B_- e^{\lambda_- t}) \quad (\text{S28})$$

Here

$$B_+ = \frac{\lambda_+ + \alpha_L}{\lambda_+ - \lambda_-}, \quad B_- = -\frac{\lambda_- + \alpha_L}{\lambda_+ - \lambda_-}, \quad \lambda_{\pm} = \frac{-(\alpha_L + \alpha_A) \pm \sqrt{(\alpha_L + \alpha_A)^2 + 4(R_0 - 1)\alpha_L \alpha_A}}{2}$$

with  $R_0 = \beta_1 / \alpha_A$ . The solution is shown for several examples in Figure S5. Note that the crossover region lasts for only a few days in this case.

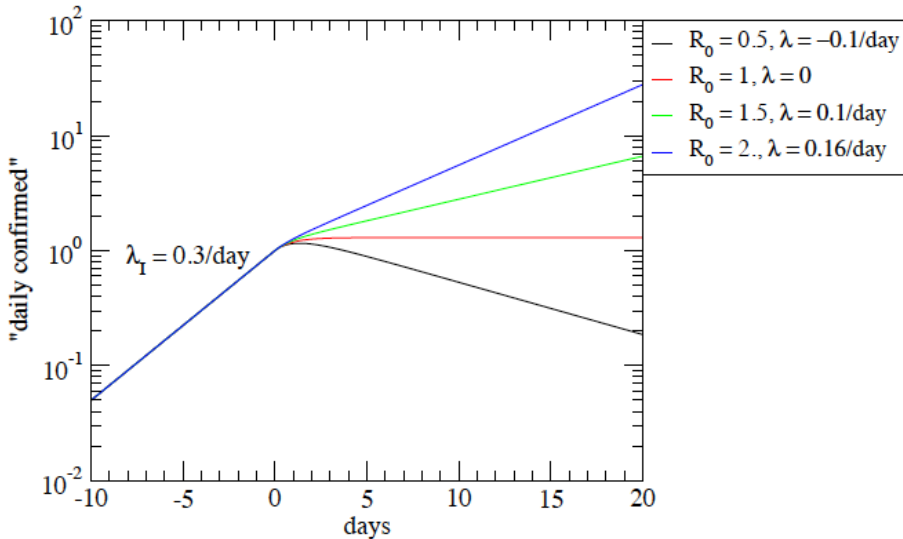


**Figure S5. Simulation of daily confirmed infections under a sudden reduction of  $\beta_{\text{eff}}$ .** The epidemic initially grows at a rate  $\lambda_i = 0.3 / \text{day}$  before the jump. Different curves correspond to different values of  $R_0$  under the new policy.

## References

- [1] Wallinga, J., Lipsitch, M. How generation intervals shape the relationship between growth rates and reproductive numbers. *Proc. R. Soc. B Biol. Sci.* 274, 599–604 (2007).
- [2] Men, K. *et al.* Estimate the incubation period of coronavirus 2019 (COVID-19). *medRxiv* 2020.02.24.20027474 (2020). doi:10.1101/2020.02.24.20027474
- [3] Xia, W. *et al.* Transmission of corona virus disease 2019 during the incubation period may lead to a quarantine loophole. *medRxiv* 2020.03.06.20031955 (2020). doi:10.1101/2020.03.06.20031955
- [4] Du, Z. *et al.* The serial interval of COVID-19 from publicly reported confirmed cases. *medRxiv* 2020.02.19.20025452 (2020). doi:10.1101/2020.02.19.20025452.